Electroplating of selective surfaces for concentrating solar collectors

Erik Zäll[1], Andreas Nordenström[1], Jonatan Mossegård[2] and Thomas Wågberg[1]

[1] Umeå University, Umeå (Sweden)

[2] Absolicon Solar Collector AB, Härnösand (Sweden)

Abstract

A spectrally selective surface is produced by electrodeposition of a Co-Cr coating on a stainless steel substrate. The plating bath consisted of $CrCl_3 \cdot 6H_2O$ and $CoCl_2 \cdot 6H_2O$ dissolved in a deep eutectic solvent (DES) of choline chloride and ethylene glycol. This DES enables the use of trivalent (Cr(III)) instead of hexavalent chromium (Cr(XI)) which significantly reduces health risks associated with chromium electroplating. The selective surface exhibits an absorptance (α) of 0.96 and an emittance (ϵ) of 0.13 at 100°C making it well adapted for mid- to low-temperature concentrating solar collectors. The 1.8 μm thick coating exhibits a porous structure on the surface as well as throughout the entire coating. The surface of the coating comprises of Co oxides and hydroxides, while the bulk consists of metallic and oxidized Co and only small fractions of Cr compounds. Initial tests of the thermal stability indicate that the coating does not maintain optical properties at an acceptable level over a lifetime of 25 years. At approximately 438°C significant parts of the coating is oxidized in an oxygen rich environment.

Keywords: spectrally selective coating, Co-Cr coating, electroplating, absorptance, emittance, surface structure

1. Introduction

Electroplating is an old and well established technique that has been used to produce selective surfaces for solar collectors since at least 1970 (Selvakumar & Barshilia, 2012). Several metals, including nickel, cobalt and chromium, have been used to electroplate selective surfaces. Black chromium exhibited the best optical properties and as a result electroplated black chrome became one of the most commonly used selective surfaces (Abbas, 2000). However, conventional electroplating of chromium is being legally restricted because it is based upon solutions containing Cr(XI) in the form of chromic acid which is carcinogenic and toxic (Zhang, et al., 2015). As a result, the black chrome has largely been replaced by selective coatings produced with different physical vapor deposition (PVD) techniques. These coatings are competitive in terms of both optical performance as well as durability (Selvakumar & Barshilia, 2012). But the demand for advanced equipment makes the production of these coatings costly. Hence, efforts are being made to amend the health related issues associated with the black chrome coatings by replacing the Cr(XI) with Cr(III) in the electroplating bathes.

In this work, a spectrally selective Co-Cr coating is produced. The coating is electroplated using Cr(III) which is enabled by the DES based electrolyte used, significantly reducing the health related issue.

2. Theory

When evaluating the degradation of the optical properties of a selective coating the following performance criteria function (PC) is used

$$PC = -(\alpha_f - \alpha_i) + x(\epsilon_f - \epsilon_i), \qquad (1)$$

where indices f and i indicates represents properties after (final) and before (initial) exposure to the degradation test. The parameter x is a weighting factor used to adjust for the fact that absorptance and emittance does not affect the optical performance of the selective surface equally. Both the working temperature, irradiance and the concentrating factor of a collector affects the weighting factor. In this case the selective coating is intended for a parabolic trough collector with glass covering the entire trough, which results in

$$x = \frac{d\pi\sigma(T_s^4 - T_{amb}^4)}{\tau\rho b I_{dir}}, \qquad (2)$$

where d is the diameter of the receiver pipe, σ is the Stefan–Boltzmann constant, T_s is the surface temperature of the receiver pipe, T_{amb} is the ambient temperature, τ is the transmittance of the cover glass, ρ is the reflectance of the reflector, b is the width of the aperture area and I_{dir} is the direct solar irradiance. While a weighting factor can be used to evaluate a selective surface with regards to a certain collector or conditions, the selectivity (S) is often used to evaluate a selective surface in general. The selectivity is given by

$$S = \frac{\alpha}{\epsilon}. \tag{3}$$

When constructing an aging test for a selective surface intended for a solar collector, the effective temperature (T_{eff}) is necessary to introduce. T_{eff} is necessary to relate a certain number of years of use at a certain working temperature, to the conditions and time of an accelerated aging test. For more information about the effective temperature of a solar collector see *Qualification test procedure for solar absorber surface durability* by Carlsson et al. (Carlsson, et al., 2000). In the case with of a solar collector with a controlled working temperature of 160°C it is given by

$$e^{\frac{-E_T}{RT_{eff}}} = \frac{2800 e^{\frac{-E_T}{R(433K)}} + e^{\frac{-E_T}{R(333K)}}}{8760}, \tag{4}$$

where E_T is the Arrhenius energy of the surface and R is the ideal gas constant.

3. Experimental

The plating process was conducted with a working electrode (WE) of stainless steel (AISI 304) and a titanium mesh, coated with noble metal oxides, as a counter electrode (CE). Prior to deposition the substrate was sonicated in acetone for 15 minutes, electropolished and submerged in a 13 wt% HCl solution. The electropolishing process was performed according to the method developed by Lin & Hu to ensure an as smooth and clean surface as possible (Lin & Hu, 2008). The electrolyte consisted of $CrCl_3 \cdot 6H_2O$ and $CoCl_2 \cdot 6H_2O$ with a molar ratio of 2:1, dissolved in a DES of ethylene glycol and choline chloride with a molar ratio of 16:1.

The parameters used for the electroplating process was determined in a report by Andreas Nordenström using the design of experiment method[1]. The optimization was conducted with the intention of optimizing the coating for applications in Absolicon's T160 model. As a result, a weighting factor calculated with equation 2 for the T160 model at 160°C was used (x=0.16) resulting in the importance of the emittance being much lower than if the more conventional selectivity, see equation 3, was used.

The electroplating was conducted using chronopotentiometry for 10 minutes with the electrolyte kept at a temperature of 44°C. The electrolyte was stirred prior but not during the deposition to ensure a homogenous distribution in terms of salt concentration as well as temperature without disrupting the deposition process. The current density (CD) used was 9.2 mA/cm^2 for the coating optimized for the T160 and 8 mA/cm^2 for the coating with the highest selectivity. When necessary samples coated with 9.2 and 8 mA/cm^2 are called S_9.2 and S_8.0 respectively. Whenever this distinction is not made the sample in question is one deposited with a CD of 9.2 mA/cm^2.

To determine the optical properties the reflectance was measured in the region 0.3 – 23 μm. A Perkin Elmer 900 spectrophotometer with a 15 cm diameter integrating sphere for the UV/Vis/NIR region (0.3 – 2.5 μm) and a Bruker fourier transform infrared spectroscope for the IR region (2.5 – 23 μm). The direct 1.5 AM solar spectrum provided by the National renewable energy laboratory (NREL, 2018) was used to calculate the α, and ϵ was calculated at 100°C using the blackbody spectrum. The surface and cross section of the coating was investigated using scanning electron microscopy (SEM). The cross section was revealed using a focus ion beam (FIB) to mill a ramp into the surface of the coating. The chemical composition was investigated using X-ray photoelectron spectroscopy (XPS) and Energy-Dispersive X-ray spectroscopy (EDX).

The thermal stability of the selective surface was evaluated with a method that was based upon a standardized test for selective surface in flat plate solar collectors developed in task X (Carlsson, et al., 2000), but slightly adjusted to adopt to selective surfaces in concentrating solar collectors after conversation with Stefan Brunold at the SPF institute for solar technology. The adjustments consisted of altering the test temperature to 320°C, using an

---

[1] Nordenström, A., 2018. *Investigating an electroplating method of Co-Cr alloys - A design of experiment approach to determine the impact of key factors on the electroplating process*, Master Thesis, Umeå University

effective temperature derived with equation 4 and using a weighting factor (equation 2) adapted for the relevant parabolic trough collector. The Arrhenius energy was assumed to be 50 kJ/mol and the test was conducted by exposing samples to 320°C in a muffle furnace and removing them from the furnace successively to investigate the degradation of the optical properties using equation 1. The weighting factor (x) given by equation 2 was calculated with $T_s = 100°C$ giving $x = 0.06$. Two samples, S1 and S2 were investigated after 43 and 136.4 hours in the furnace respectively.

The thermal degradation of the coating was further investigated by us of thermogravimetric analysis (TGA). Two runs of TGA was performed, where the first was conducted at 2 °C/min up to 1000°C in a nitrogen atmosphere flowing at 40 cm³/min. The second one was conducted at 10 °C/min up to 900°C in an oxygen atmosphere flowing at 40 cm³/min

4. Result & Discussion

The reflectance of the coating presented with the 1.5AM Direct solar spectrum and the 100°C black body spectra can be seen over the interval 0.3 – 23 μm in figure 1. Both samples exhibit strongly selective properties with α = 0.961 and ε = 0.149 for sample S_9.2 and α = 0.958 and ε = 0.131 for sample S_8.0. As mentioned previously, this results in S_8.0 having the highest selectivity with S = 7.31. The optical properties make it suitable for a low- to mid-temperature concentrating solar collectors where the absorptance is of greater importance than the emittance.
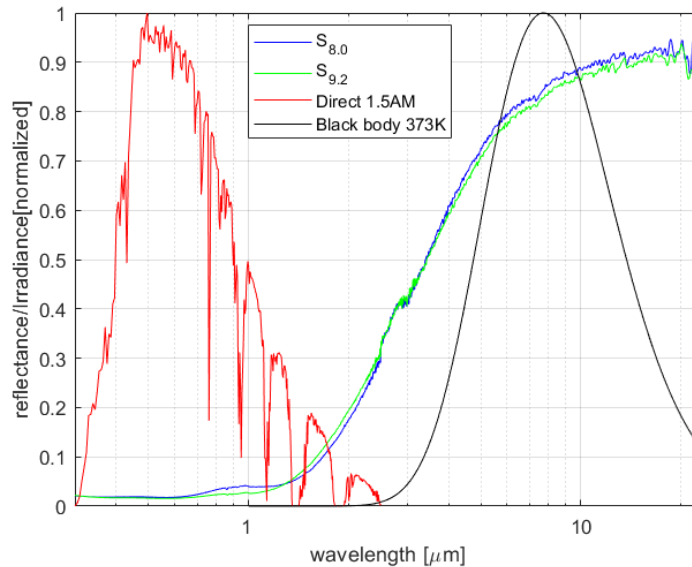

Fig. 1: Reflectance spectra of sample S_8.0 and S_9.2 presented with the direct 1.5 solar spectra and the 100°C black body spectra.

The reflectance spectra follow the expected general appearance of a selective surface with very low reflectance (roughly 0.02) in the UV range, a transition to highly reflective starting at 1.5 μm and a reflectance of above 0.8 from 5 μm and upwards. The only things that deviate from this is a local maximum, that is more pronounced for S_8.0 than S_9.2, at roughly 1 μm and the fact that the transition between instruments is not perfect. The spectra from the UV/Vis/NIR and the FTIR does not overlap perfectly as the spectra from the aforementioned instrument is a bit higher at the transition at 2.5 μm. This mismatch is not large and if anything, it would indicate that the optical properties are better than presented here as the UV/Vis/NIR spectra and FTIR spectra would have to be moved down respectively up to correct for it.

The absorptance is competitive compared to many selective surfaces in literature where only the best coatings reach an absorptance above 0.95 (Atkinson, et al., 2015) (Kennedy, 2002). It is however possible to achieve up to α = 0.99 with a chromium coating produced with similar method (Surviliene, et al., 2014). It is however unclear what the emittance of this exceptionally absorbing coating is, especially considering that optimizing one of the optical properties to the extreme often comes at the expense of the other.

Considering that the substrate is polished stainless steel (ε = 0.093) an achieved emittance in the region 0.13 – 0.15 is in line with best expectations. This is because the low emittance of these kinds of surfaces are generated by having a substrate with low emittance and the coating being close to transparent in the IR region. Hence, the

emittance can never be lower than the substrate itself and is typically higher because the coating isn't completely transparent. This makes the pretreatment of the surface as well as the thickness of the coating key aspects in achieving a surface with a low emittance.

4.1. Structure of the coating

Investigation of the surface with SEM shows a surface with structures resembling sheets with cavities in between, see figure 1. The length and thickness of the sheet-like surface structures varies, but a rough estimate of an average is 1 μm long and 0.1 μm thick. No reoccurring pattern can be seen in the orientation of the structures, but the surface is very homogeneous (more visible when less magnified) and does not exhibit any cracks.

Based upon the look of the surface it is plausible to assume that the absorptance of the coating is at least partly generated by the use of surface texture, where a structure generating multiple reflections within the structure to generate a higher absorptance that the intrinsic absorptance of the material itself (Testafamichael, 2000). For this to work the size of the structures determines which wavelengths are absorbed. If the wavelength is much longer than the structures on the surface the light will not reflect multiple times and the absorptance is lower, this is how the surface can maintain a high reflectance in the IR spectra.

It has been observed that the CD strongly affect the size of the surface structures of the finished coating, with the correlation being that a higher CD gives larger surface structures. Hence, a higher CD gives higher absorptance of longer wavelengths. Likely, the local reflectance maxima at 1 μm is more pronounced for S_8.0 because it was applied with a lower CD and hence can be expected to exhibit smaller surface structure.
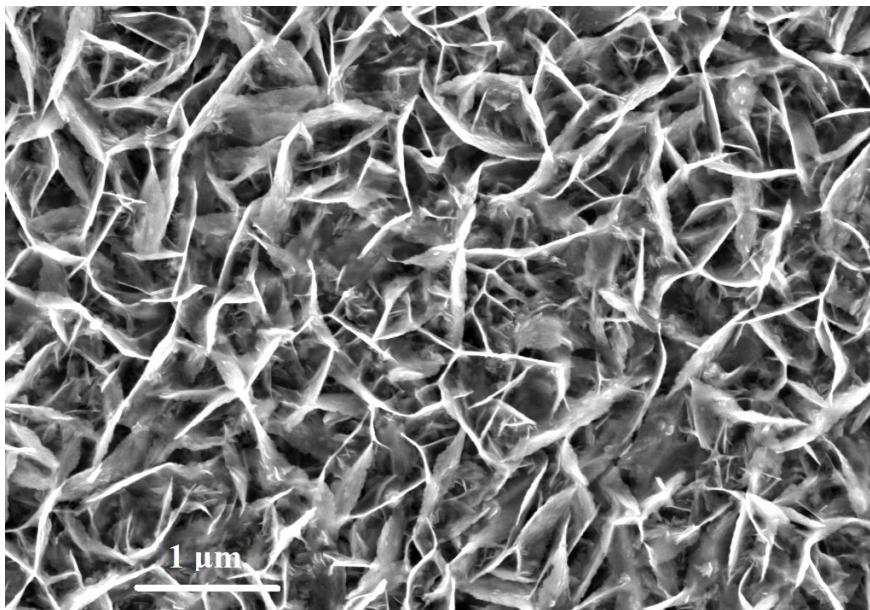

Fig. 2: SEM image of the surface of the Co-Cr coating.

A SEM image of the cross section (CS) of the coating (exposed by use of FIB) can be seen in figure 3. The coating is approximately 1.8 μm thick and there are cavities throughout the entire coating. According to literature, the optimal thickness of a coating of this kind is 0.5-2 μm (Eugénio, et al., 2011). While there is no guarantee that this is at all true for this coating, there might be room for improvement by decreasing the thickness and thereby lowering the emittance without reducing the absorptance.
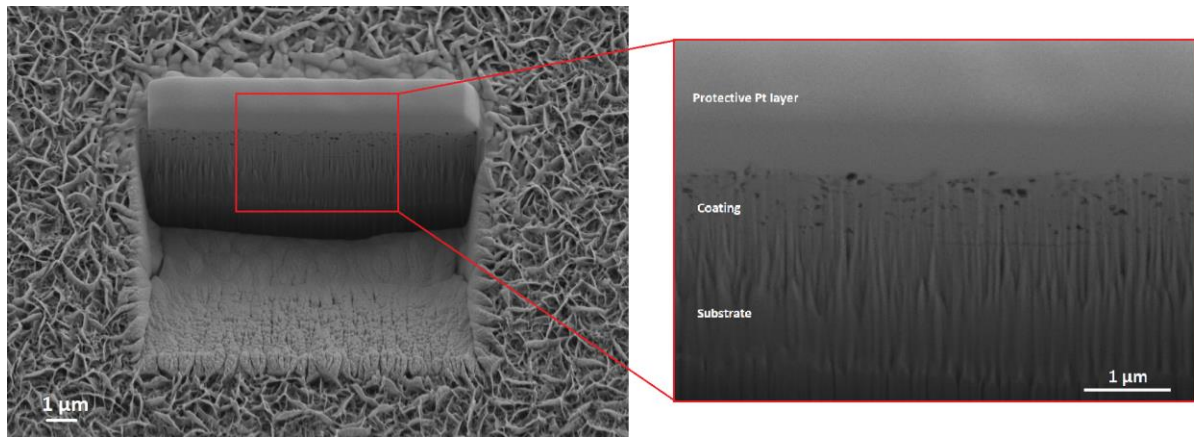
Fig. 3: SEM images of the ramp milled down into the surface of the coating (left) and the exposed cross section of the coating (right).

4.2. Chemical composition

The XPS measurements, the result of which can be seen in table 1, shows that the surfaces mostly consist of Co compounds. Almost 70 % (69.64 %) of the signal is associated with cobalt bonds with Co = O, Co – OH and Co(III) compounds constituting 26.36, 17.42 and 25.86 at% respectively. There is also a small amount of Cr (0.26 at%) in the form of Cr(III) compounds, but there are neither Co or Cr in the form of metal. At least in the case of Co this is expected as Co exposed to air at room temperature a thin layer of Co hydroxide (Co(OH)2) is formed within seconds (Tompkins & Augis, 1981). The carbon is mainly contributed to pollution from the atmosphere.

Tab. 1: XPS results on the surface of the selective surface.

C1s			O1s		
Bond	Be, eV	AC, at%	Bond	Be, eV	AC, at%
C-(C,H)	284.6	17.84	Co=O	529.7	26.36
C-O	286,2	2.71	Co-OH	531.1	17.42
COOH	287.9	2.82	C=O	532.2	5.25
CO_3^{2-}	289.2	1.02	C-OH	533.3	1.46

Co 2p 3/2			Cr 2p 2/3		
Bond	Be, eV	AC, at%	Bond	Be, eV	AC, at%
Co(III)	779,5	25.86	Cr(III)	576.2	0.26

The result of the EDX investigation of the surface as well as CS of the coating is presented in table 2. The most abundant element in the coating is Co considering the 62.3 and 63.1 at% readings from the surface and CS of the coating. The form of the Co is however not as clear. Considering that there should not be any Fe in the coating, the fact that the surface scan has a 1.3 at% reading of Fe means that the penetration depth is all the way through the coating to the substrate. This means that the oxygen reading can't be entirely from the surface oxides/hydroxides apparent in the XPS results, but that there are some Co oxides and hydroxides in the coating as well. However, considering the low level of oxygen compared to Co there is most likely also metallic Co in the coating.

Tab. 2: Result of the EDX investigation of the coating presented in at%.

Area\Element	C	O	Cl	Cr	Fe	Co	Mn	Ni	Ga	Pt
Surface	15.4	17.7	0.7	2.3	1.3	62.3				
CS coating	8.8	0.8	0.2	6.7	16.5	63.1		1.2	1.8	0.9
CS substrate	3.2	0.2		19.1	66.9	2.3	1.3	5.9	0.9	0.3

Considering that the substrate (stainless steel AISI 304) contains a large amount of Cr the reading on the surface and in the coating CS has to be compared to other components of the substrate to determine if there is some Cr in the coating or if the Cr readings are all results of the Cr in the substrate. If we compare the ratio between Cr and Fe (Cr/Fe) for the three readings we get 0.29, 0.41 and 1,77 for the substrate (note that 19.1 and 66.9 at% is within the concentrations for Cr and Fe in AISI 304 according to specification), coating and surface respectively. By doing this it becomes clear that the Cr reading is not a result of the content in the substrate but rather that there are Cr in the coating. It is however not possible to determine that there are more Cr towards the surface based upon the results since the 25° angle used when performing the EDX of the coating CS causes that reading to penetrate deeper into the substrate than the reading on the surface.

The fact that there are Cr in the coating is supported by the fact that removing the Cr(III) component in the electrolyte results in a layer of reduced Co on the WE with extremely poor adhesion, it falls of when rinsing after deposition. This indicates that the Cr plays an important role in the initial steps of the deposition process at the very least. This together with the small amount of Cr at the surface according to the XPS results indicates that the Cr concentration is rather higher at the substrate and that there is a negative concentration gradient towards the surface of the coating.

The CS was also investigated with EDX mapping, the result of which can be seen in figure 4. In the picture showing the distribution of Co it is clearly visible that it is limited to the coating, where it also is abundant as expected. The Fe and Cr on the other hand has the strongest signal from the substrate, but they differ in the way that the Cr concentration does not decrease as abruptly at the transition to the coating. While still being clearly lower than in the substrate, there is also Cr in the coating, however at a relatively low concentration. The oxygen does not show as abrupt changes in the concentration, but it shows a distinct positive gradient towards the surface of the coating.
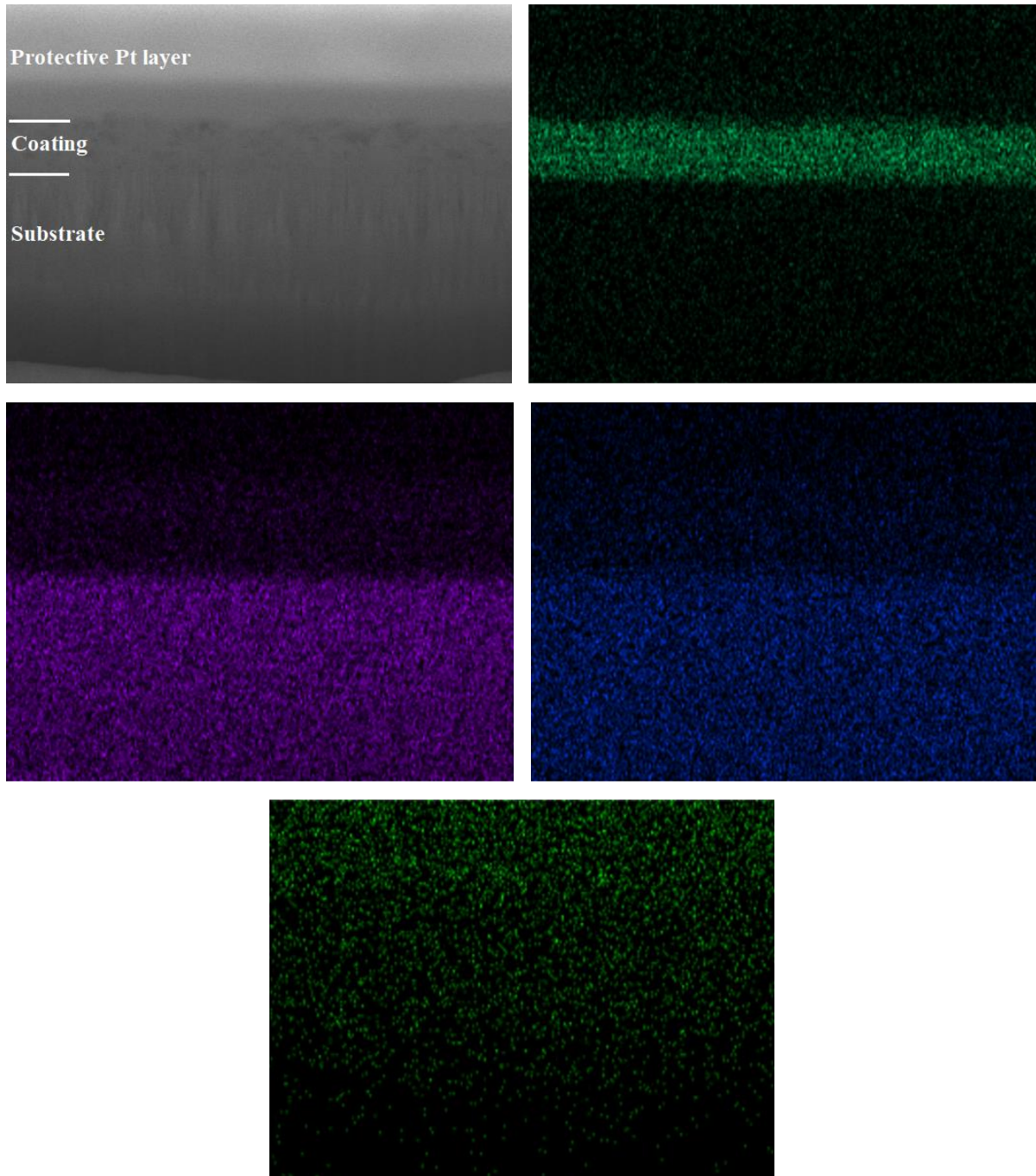
Fig. 4: SEM of the cross section (upper left) and EDX mapping of the cross section divided after the elements Co (upper right), Fe (middle left), Cr (middle right) and O (bottom).

4.3. Thermal stability

The result of the thermal stability test can be seen in table 3. The degradation in terms of optical performance after a simulate lifetime of 0.63 and 2 years respectively is PC = 0.023 and 0.081. Using a polynomial fit of only those two data points gives a degradation of 0.05 after a simulated lifetime of 0.95 years. Considering that the 5 % degradation is the limit for what is acceptable over a 25-year lifetime the coating has clearly failed the test.

Tab. 3: Result of the thermal stability test performed at 320°C in a muffle furnace.

Sample	Time in furnace [h]	Simulated Lifetime [years]	PC
S1	43	0.63	0.034
S2	136.4	2	0.10

The reflectance spectra over the interval 0.28 – 1.1 μm of two samples, S1 and S2, before and after being exposed to a high temperature can be seen in figure 5. The reflectance of the tow samples after the test is very similar, almost perfectly overlapping, over the interval 0.28 – 0.8 μm, but S2 had a lower reflectance initially giving it a greater degradation. It is unclear if the reflectance the two samples exhibit in this region after the test is a stable level from which the degradation does not continue, or if the fact that they align is a coincidence caused by the initial difference in the reflectance. In the region 0.8 – 1.1 μm on the other hand, the two samples exhibit very different reflectance. S1 having ha peak and a trough at roughly 0.87 and 1.01 μm respectively, while S2 have a peak at roughly 0.99 μm before declining sharply towards the edge of the registered spectra (1.1 μm). A possible explanation to the differences in this region is a gradual degradation of the surface structures of the samples, changing how efficiently they capture the light in these wavelengths.
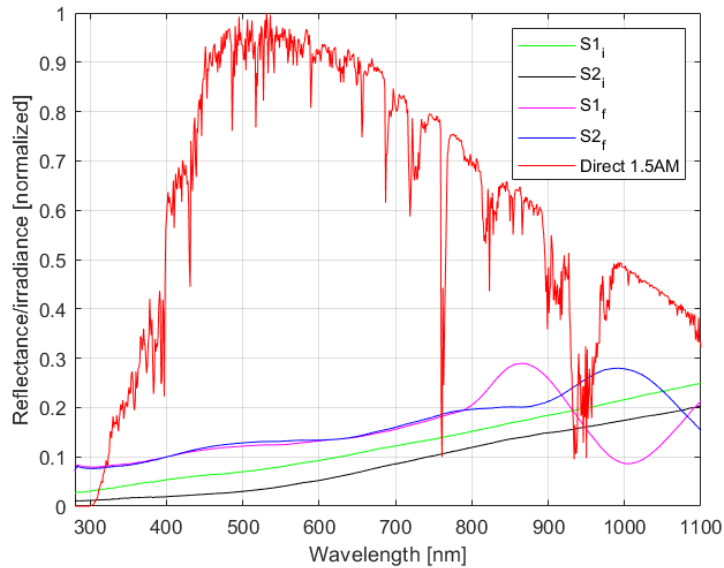

Fig. 5: Reflectance of two samples before (i) and after (f) aging tests presented with the 1.5AM solar spectra.

The result of the TGA performed in a nitrogen and an oxygen atmosphere can be seen in figure 6 and 7 respectively. The nitrogen run reveals a gradually decreasing weight to approximately 400°C before it gradually increases for the rest of the test. The absence of transformation peaks at 30, 252 and 800°C reveals that the samples do not contain $Co(OH)_2$, CoOOH or Co_3O_4 there would be distinct reactions at 130, 252 and 800°C respectively (Yang, et al., 2010).

The TGA performed in air reveals a small reaction at 331°C that could be contributed to a small amount of cobalt carbonate decomposing to Co_3O_4 (Ei, et al., 1996). This is supported by the small reading of carbonate in the XPS results. The largest reaction reaction visible is however an oxidation centered around 438°C at which the weight of the sample increases from 95 to 116 % of the original weight, resulting in a 22 % increase in weight. This indicates an oxidation of a big part of the sample. One possibility is that there is large amount of metallic Co available that is oxidized to Co_3O_4, and that cobalt (II)oxide is what starts to decomposes to CoO at 850°C (Ei, et al., 1996) causing the drop in weight between 850 and 900°C.
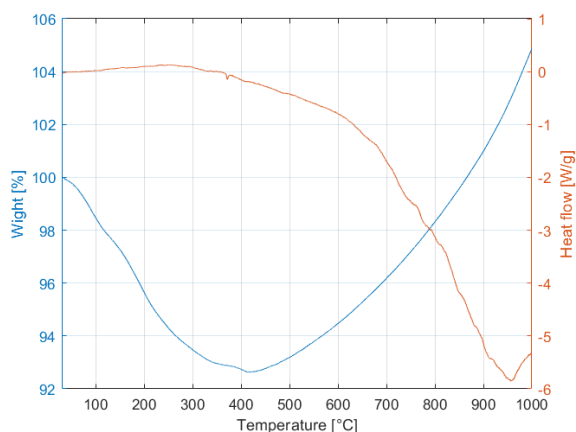
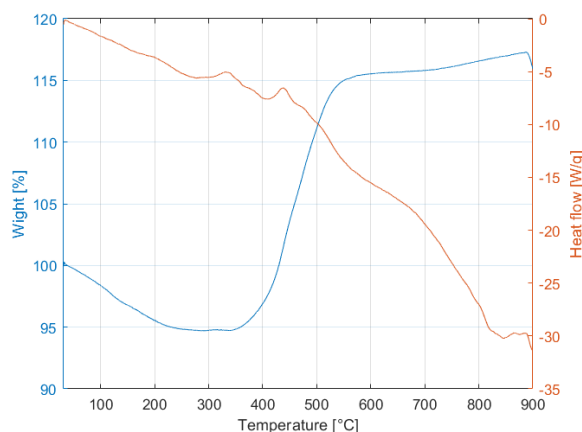**Fig. 6: TGA data for the coating in a nitrogen atmosphere.**

Fig. 7:TGA data for the coting in an air atmosphere.

3.2. General discussion

As previously discussed, the CD is central for important aspects of the coating, like thickness and surface structure. Because of this it must be mentioned that all the depositions in this project has been conducted in an electrochemical cell where both CE and WE are flat electrodes. As a result, only one side of the WE were facing the CE during the deposition. As a result, there is an uncertainty in the actual CD of the side facing the CE because the amount of the side facing away from the Ce that is electroplated varies between samples. As expected, a higher CD results in a larger part of the "back" of the WE that is being electroplated. It should be noted that the amount of the "back" that is plated is small, roughly 10-20 %. Since the CD mentioned in this report is calculated using the area of the side of the WE that face the CE it is an overestimation, however it not large.

5. Conclusions

The electroplated surface is strongly selective as α and ϵ are 0.96 and 0.13 respectively, giving a selectivity of S = 7.4. These optical properties make the surface suitable for a low- to mid-temperature concentrating solar collector. The selective Co-Cr coating is 1.8 μm thick and exhibits a porous structure throughout the coating and has a surface structure resembling sheets around 1 μm long with cavities between. The surface of the coating is covered in Co oxides and hydroxides, while the bulk of the coating consists of Co in the form of both metallic and oxidized Co and only a small fraction of Cr compounds. Initial tests of the thermal stability indicate that the coating does not maintain optical properties at an acceptable level over a lifetime of 25 years and that a large part of the coating is oxidized at approximately 438°C in an oxygen rich environment.

6. Future works

Based upon the result of the DoE optimization done there are room for improvement in terms of optimization with regards to the optical properties[1]. However, considering that the optical properties are already at a competitive level, the focus of the work going forward will be the problem with thermal stability. Initially by thoroughly evaluating the degradation process to determine which reactions cause the degradation and under which circumstances. After that efforts to increase the thermal stability can be made.

One way to increase the thermal stability could be to apply a protective layer on top of the selective coating that is also anti reflective increasing the absorptance of the surface. This has been successfully done with a AlOOH coating on a selective surface of carbon nano tubes with (Bera, et al., 2016).

It could also be possible to oxidize the Co-Cr in a controlled manner, increasing the stability of it by changing the Co compounds to Co_3O_4 while keeping the surface structure of the coating. Either through electrolytical oxidation at room temperature, or by exposing it to a temperature and an atmosphere adapted to oxidize the sample without ruining the optical properties.

---

[1] Nordenström, A., 2018. *Investigating an electroplating method of Co-Cr alloys - A design of experiment approach to determine the impact of key factors on the electroplating process*, Master Thesis, Umeå University

It is also possible to use a highly reflective undercoating of nickel to prevents diffusion from the substrate to the coating. This also lowers the emittance of the substrate potentially increasing the selectivity of the finished surface.

7. Acknowledgements

8. References

Abbas, A., 2000. Solchrome solar selective coatings - an effective way for solar water heates globally. Renewable Energy, Volym 19, pp. 145-154., Avaliable from: doi: 10.1016/S0960-1481(99)00028-2.

Atkinson, C., Sansom, C. L., Almond, H. J. & Shaw, C. P., 2015. Coatings for concentrating solar systems - A review. Renewable and Sustainable Energy Reviews, Volym 45, pp. 113-122. , Avaliable from: doi: 10.1016/j.rser.2015.01.015.

Bera, R. K., Mhaisalkar, S. G., Mandler, D. & Magdassi, S., 2016. Formation and performance of highly absorbing solar thermal coating based on carbon nanotubes and boehmite. Energy Conversion and Management, Volym 120, pp. 287-293., Avaliable from: doi: 10.1016/j.enconman.2016.04.081.

Carlsson, B., Möller, K., Köhl, M., Frei, U., Brunold, S., 2000. Qualification test procedure for solar absorber surface durability. Solar Energy Materials and Solar Cells, 61(3), pp. 255-275. , Avaliable from: doi: 10.1016/S0927-0248(99)00111-7.

Ei, G. A., Ahmad, A. S., Ai, A. N. & Ei, H. G., 1996. TI ~ . RMAL DECOMPOSITION OF BASIC COBALT AND COPPER CARBONATES Thermal stability of the produced oxides as influenced by. October, Volym 46, pp. 1801-1808., Avaliable from: doi: 10.1007/BF01980784.

Eugénio, S., Rangel, C. M., Vilar, R. & Botelho Do Rego, A. M., 2011. Electrodeposition of black chromium spectrally selective coatings from a Cr(III)-ionic liquid solution. Thin Solid Films, 519(6), pp. 1845-1850., Avaliable from: doi: 10.1016/j.tsf.2010.10.029.

Kennedy, C. E., 2002. Review of Mid- to High- Temperature Solar Selective Absorber Materials Review of Mid- to High- Temperature Solar Selective Absorber Materials, u.o.: u.n.

Lin, C.-C. & Hu, C.-C., 2008. Electropolishing of 304 stainless steel: Surface roughness control using experimental design strategies and a summarized electropolishing model. Electrochimica Acta, 53(8), pp. 3356-3363., Avaliable from: doi: 10.1016/j.electacta.2007.11.075.

NREL, 2018. nrel.gov., [Online] Available at: https://www.nrel.gov/grid/solar-resource/spectra-am1.5.html, [Accessed 05 09 2018].

Selvakumar, N. & Barshilia, H. C., 2012. Review of physical vapor deposited (PVD) spectrally selective coatings for mid- and high-temperature solar thermal applications. Solar Energy Materials and Solar Cells, Volym 98, pp., Avaliable from: doi: 1-23.10.1016/j.solmat.2011.10.028.

Surviliene, S., Cesuniene, A., Juskenas, R., Selskiene, A., Bucinskiene, D., Kalinauskas, P., Juskevicius, K., Jureviciute, I., 2014. The use of trivalent chromium bath to obtain a solar selective black chromium coating. Applied Surface Science, Volym 305, pp. 492-497., Avaliable from: doi: 10.1016/j.apsusc.2014.03.122.

Testafamichael, T., 2000. Characterization of Selective Solar Absorbers. u.o.:u.n.

Tompkins, H. G. & Augis, J. A., 1981. The oxidation of cobalt in air from room temperature to 467°C. Oxidation of Metals, 16(5-6), pp. 355-369., Avaliable from: doi: 10.1007/BF00611349.

Yang, J., Liu, H., Martens, W. N. & Frost, R. L., 2010. Synthesis and Characterization of Cobalt Hydroxide. Physical Chemistry, 114(7), pp. 1-11.

Zhang, J., Gu, C., Tong, Y., Gou, J., Wang, X., Tu, J., 2015. Microstructure and corrosion behavior of Cr and Cr–P alloy coatings electrodeposited from a Cr(III) deep eutectic solvent. RSC Adv., 5(87), pp. 71268-71277., Avaliable from: doi:10.1039/C5RA13056E.